Quantum Computing with Quantum Dots

Joon Ho Baek, Happy Hsin, Joshua LaForge, Daniel Nedelcu

August 13, 2004

Abstract

Our time at the Computing Beyond Silicon Summer School, hosted by Caltech, gave us a unique opportunity to explore new concepts and learn about advances in modern information processing that interest us. We chose to study quantum computation using quantum dot systems because of their potential for bringing forth a solid-sate quantum information processing system. Specifically we chose to investigate three questions: (1) What physical properties of a quantum dot can be used to carry quantum information? (2) How do we create quantum gates using these systems? (3) How do we create simple quantum circuits using these systems? This paper presents what we have discovered for three types of systems: exciton systems, electron spin systems, and nuclear spin systems. We also investigate the role that polarons play in the decoherence of spin systems.

1 Introduction

Interest in quantum computation was sparked when the algorithms of Shor [1] and Grover [2] demonstrated that computational hard problems on a classical computer become feasible on a quantum computer. Investigations into a physically realizable quantum computer have been carried out on ion-trap systems [3, 4], as well as cavity quantum electrodynamic systems [5], and in nuclear magnetic resonance systems [6].

While the knowledge gained from research is beneficial to our understanding of quantum information processing systems, it is unclear if such systems will be able to scale up to the large-scale systems that will be needed if quantum computers are ever to become more than an academic curiosity, or highly specialized computational tool. It is speculated that a scaleable, and economically feasible, quantum information processing will be created with solid-state systems. It may be that solid-state quantum information processing will come to dominate the field of quantum computation as it has with classical computational systems with the microelectronic circuit.

For this paper we chose to investigate the potential applications that quantum dot systems, one class of solid-state systems, may have for quantum information processing. Specifically we set out to investigate three questions:

- What physical properties of a quantum dot can be used to carry quantum information?
- How do we create quantum gates using these systems?
- How do we create quantum circuits using these systems?

As a corollary to answering these questions we will also explore how the systems we study fulfill DiVincenzo's requirements for an operable quantum computer [7]. These five requirements are as follows: (i) identification of well-defined qubits, (ii) reliable state preparation, (iii) low decoherence, (iv) accurate quantum gate operations, and (v) strong quantum measurements.

We chose to study three separate systems for information processing in quantum dots: exciton systems, electron spin systems, and nuclear spin systems. What we have learned about these systems will be reported in this paper.

1.1 Quantum Computation

Quantum computers store information in two-level quantum systems and manipulate information by precisely controlling the system's Hamiltonian. Typically, the fundamental unit of information in a quantum computer is referred to as a qubit, despite attempts to point out how grotesque a misuse of the english language this name is [8].

Information processing is performed on an array of qubits through a series of two-qubit and single-qubit gates. This process is similar to how boolean bits are operated on by logic gates in classical computing. There are several quantum logic implementations which have been shown to provide a universal set of gates for computation, and these will be discussed for the separate systems.

In order for the computation to proceed the system of qubit states must evolve coherently. Therefore a fine balance between isolating the system from the environment to maintain coherence, and coupling to the system to allow control of the evolution must be achieved. Maintaining coherence of the qubit states has proven to be a difficult problem to solve, but fortunately there are schemes of active quantum error correction that are able to maintain the coherence of the qubits for a certain cost in computational overhead. It is estimated that in order to maintain coherence using quantum error correction for larger arrays of qubits, that the gate delay (or time it takes one gate to operate) must be on the order of 10^4 times shorter then the decoherence times of the individual qubits [9].

1.2 Quantum Dots

The term quantum dot is usually used to describe a semiconductor nanocrystal. Quantum dots are confined, zero-dimensional semiconductor systems created at the nanoscale. The physical boundaries of the quantum dot confine charge carriers within the material. This confinement results in properties that are not seen in the bulk form of the material. For example, silicon, which is usually a poor light emitter in its bulk form because it has an indirect-band gap, emits light when it is confined as quantum dots [10].

Figure 1: Colloidally prepared CdSe quantum dots of different sizes, demonstrates how the size of the quantum dot affects confinement and thus the optical properties of the material [11].

The confinement of the charge carriers within the quantum dot can be adjusted, thereby affecting some of the material's properties, by varying the size of the quantum dot. This effect is most spectacularly seen in the rainbow of colors that can be produced in colloidal CdSe quantum dots by varying their sizes (Figure 1).

Typically the diameter of a quantum dot (D), and thus the level of confinement that it produces, is characterized by its relation to the Bohr radius of an exciton (Hydrogenically coupled electron-hole pairs) (a_B). Strong confinement occurs when $D < 2a_B$, intermittent confinement when $D \sim 2a_B$, and weak confinement when $D > 2a_B$ [12]. The size of the quantum dot can also be characterized by the Fermi wavelength inside the host material, which is typically between 10 nm and 1 μm [13].

Quantum dots are prepared using several techniques including the following: lithography, molecular beam epitaxy, and colloidal methods. All of these methods share a common characteristic in that the quantum dot is created via a distinct material boundary. There are other methods for creating quantum dots where electrical gating is used to confine electrons in a two dimensional electron gas within a quantum well.

Systems contained within quantum dots are better isolated from the environment and have fewer internal degrees of freedom than systems with more dimensions. Both of these characteristics are useful for increasing the coherence times of the qubit states encoded within the dot, and therefore interest in the potential applications that quantum dots have for solid-state quantum computing has developed.

2 Excitons

When photons are pumped into a semiconductor, electrons are excited into the conduction band, leaving behind holes in the valence band. Binding the electrons with their hole counterparts result in bounded electron-hole pairs, or excitons. In this section, we demonstrate how a quantum computing (QC) system can be realized using localized excitons in QDs as the elementary quantum bit. According to DiVincenzo, the five requirements that must be satisfied in order to obtain a reliable QC system are: (1) a scalable system, (2) the ability to initialize qubits (3) relatively long decoherence times (longer than the gate operation times), (4) a qubit-specific read-out capability, and (5) a universal set of quantum gates [14].

We base our analysis on the simple physical system proposed by H.Kamada[15] where a linear array of quantum dots is excited by a laser while sandwiched between two metal electrodes as seen in (Figure 2). The system can easily be scaled up by adding more QDs to the array. Quantum logic gates are performed by exciting the quantum dots with multi-color lasers. In the absence of excitation and radiation, however, the QD system will fall back in the ground state thus initializing the qubit states. One main obstacle is decoherence, or the effects of uncontrollable coupling with the environment. The decoherence time for an exciton typically ranges from 20ps to 100ps, which is considerably shorter than the decoherence times of nuclear or electron spin. This is a problem since gate operations take approximately 40ps to perform. However, implementing ultrafast (femtosecond) optoelectronics will enable us to bypass this problem. Read-out on the QDs can be achieved by placing the excitation and probe beam spots on a specific location where a number of qubits with different excitonic frequencies can be accessed. The somewhat randomized distribution of the QD size and composition allow qubits with different excitation frequencies to exist, making it easier to identify specific qubits by singling out the different frequencies.

Finally, we attempt to find a universal set of gates for our system. Any universal quantum computation is a unitary operator that can be decomposed into a series of single-qubit operations and the two-qubit controlled-NOT gate [16]. Recent experiments have demonstrated single-qubit operations in the form of Rabi oscillations [17]. Although a reliable CNOT gate has yet to be developed, research has shown a high-fidelity controlled rotation (CROT gate) to be equivalent to the CNOT gate [18]. Section 2.1 will discuss in further detail the single-qubit operations, and Section 2.2 will address the theoretical CNOT gate and the experimental implementation of the CROT gate.

2.1 Single-Qubit Operations

Single-qubit operations can be represented by single-qubit rotations [19]. As mentioned before, single-qubit gates have been experimentally observed on QDs via Rabi oscillations. Rabi oscillations are the sinusoidal time evolution of the population difference in a two-level system that occurs at the Rabi frequency before the system decoheres. This population flopping phenomenon using differential transmission techniques has been observed by T.H. Stievater whose setup is outlined below [17].

2.1.1 Rabi Oscillations of Excitons in Single Quantum Dots

The QDs were first formed in a 4nm-thick GaAs layer sandwiched between two 25nm-thick $Al_{0.3}Ga_{0.7}As$ layers. Two-minute growth interruptions at each $GaAs/Al_{0.3}Ga_{0.7}As$ interface

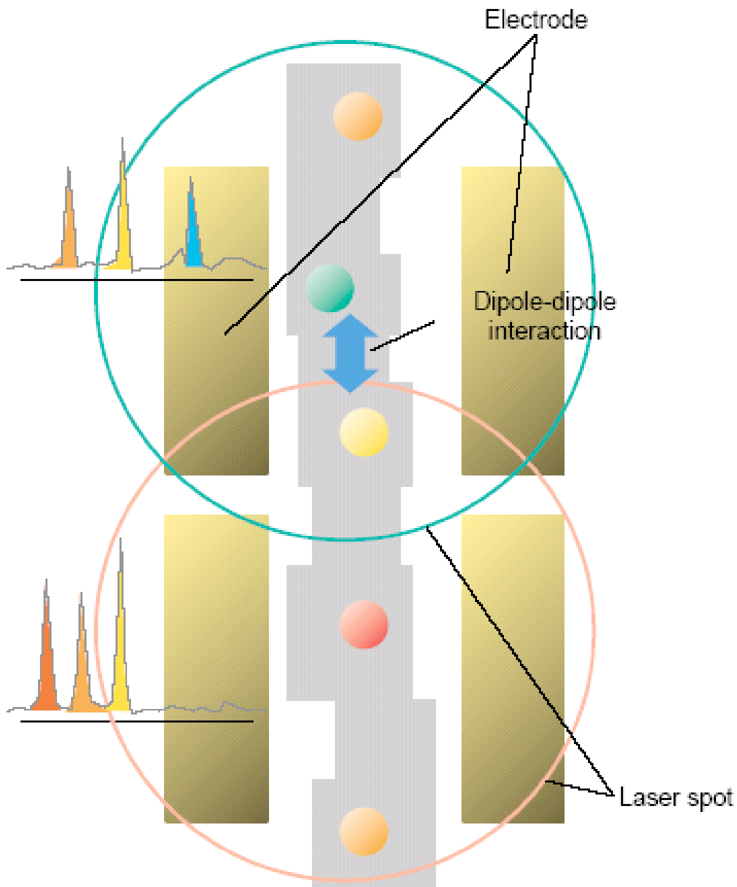

Figure 2: Linear array of quantum dots for all-optical computation. Individual QDs are accessed and distinguished by positioning the tunable laser and probe. The statistical distribution of QD characteristics enables the identity of an exciton in a particular QD to be recognized by frequency domain discrimination [15].

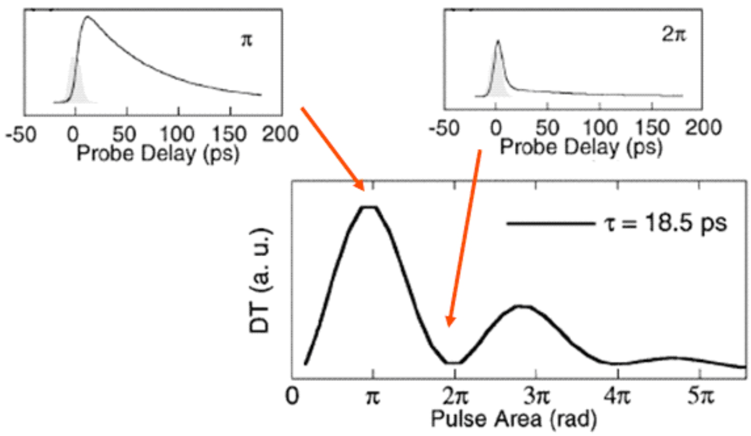

Figure 3: The calculated DT signal vs. pulse area (pump power) for $\tau = 18.5$ps and the calculated DT signal vs. probe delay for difference pump powers that correspond to pulse areas of π, and 2π [19].

created QDs with localized excitons in the GaAs layer [20, 21, 22]. The QDs were probed in low temperatures around 6K.

The experimental setup consists of a 76MHz mode-locked laser that passes through a Mach-Zehnder interferometer resulting in a pair of pulses: the pump pulse (E_1) and the probe pulse (E_2). The pump pulse is used to excite a single QD exciton while the probe pulse either increases or decreases the population depending on whether the phase of both the pulses are in phase or not. Time-integrated homodyne detection of the probe field gives rise to a differential transmission (DT) signal proportional to the level of excitation induced by the pump. Rabi oscillations were observed by fixing the delay τ between the pump and the probe and by taking the DT signal as a function of the pump power E_1, or as a function of the pulse area:

$$\Theta(t) = \mu_{eg}\epsilon_1 \int_{-\infty}^{t} E_1 t\prime dt\prime \tag{1}$$

where μ_{eg} is the electric dipole moment for the excitonic transition.

Assuming there is no dephasing, the Rabi oscillation follows $sin^2[\frac{\Theta(t)}{2}]$. In reality, however, quantum systems couple to the environment causing decoherence which decays the amplitude of the oscillation (Figure 3). The DT signal of these individual QD excitons can also be investigated by monitoring the population as a function of the probe delay, τ (Figure 3).

Depending on whether the probe pulse is in phase with the pump pulse, the population of the QD will increase (brighter luminescence) or pull back to null (vanished luminescence), thus establishing single-qubit rotations [15].

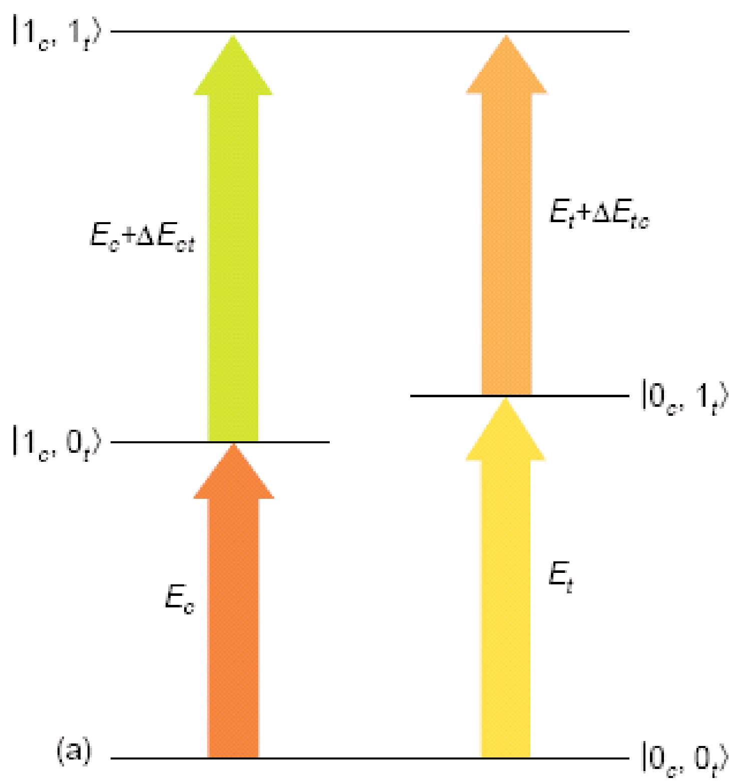

Figure 4: The CNOT gate which flips the target bit only when the control bit is 1 [15].

2.2 Two-Qubit Controlled Gates

2.2.1 The CNOT and SWAP Gates

To fulfill the universality requirement of quantum gates, a working controlled-NOT (CNOT) gate must be demonstrated. The principle of CNOT operation allows the second target bit (t) to flip only if the first control bit (c) is in the state $|1\rangle$. Figure 4 shows the energy levels for a two-qubit system. For two neighboring QDs, the presence of an exciton in one will affect the exciton energy of the other, adding ΔE_{ct} (the exciton-exciton correlation energy between dots c and t) to the single-exciton energies. Hence, by exciting the system to the state $|1_c, 0_t\rangle$, we can implement a coherent laser π-pulse (pulse with pulse area of π) with energy $E_c\prime(n_c) = E_c + \Delta E_{ct} n_c$ which will result in a π-rotation if and only if the control qubit is in the state $|n_c\rangle = |1_c\rangle$.

The calculation presented above is strictly for neighboring pairs of QDs. To perform the CNOT operation on a remote pair of QDs, we implement the SWAP gate, which switches the qubit state of one QD with the state in the adjacent QD. The SWAP gate can be achieved by performing three CNOT operations. Figure 5 shows how the remote CNOT gate is implemented. The control bit (blue) goes under the SWAP operation twice until it is adjacent to the target bit (grey). The CNOT gate is then applied the pair of the neighboring bits.

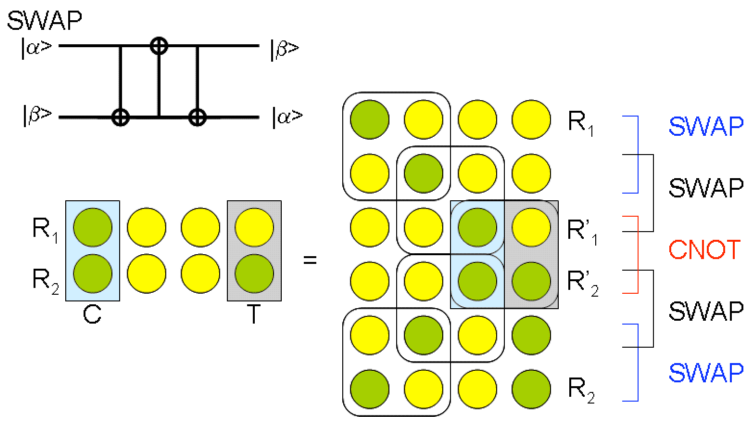

Figure 5: The SWAP gate which swaps the two input qubits. SWAP can be realized by taking three CNOT gates operations. This gate is essential when we want to perform operations on remote qubits such as the CNOT gate shown above [15].

$$\mathrm{CROT} = \begin{bmatrix} 1 & 0 & 0 & 0 \\ 0 & 1 & 0 & 0 \\ 0 & 0 & 0 & -1 \\ 0 & 0 & 1 & 0 \end{bmatrix} \qquad \mathrm{CNOT} = \begin{bmatrix} 1 & 0 & 0 & 0 \\ 0 & 1 & 0 & 0 \\ 0 & 0 & 0 & 1 \\ 0 & 0 & 1 & 0 \end{bmatrix}$$

Figure 6: The CROT gate and the CNOT gate. The two operations are equivalent under the universality requirement.

2.2.2 The Experimental Control-ROT Gate

The CNOT gate is essential for quantum computation and entanglement, however, reliable proof of one has yet to exist. In 2003, a high fidelity (reliable) controlled-rotation (CROT) gate was demonstrated [18]. The CROT gate is equivalent to the CNOT gate (except for a sign difference) (Figure 6) and can replace the CNOT gate in the universality clause [23]. Unitary rotations like the CROT gate are much easier to realize than the CNOT gate.

In the experiment done by X.Li et al, the QDs were formed naturally in a 4.2nm-thick layer of GaAs sandwiched between two 25nm-thick $Al_{0.3}Ga_{0.7}As$ barriers [23]. Linearly polarized light was used to excite the state of the QDs to the excitonic states $|0_c, 1_t\rangle$ and $|1_c, 0_t\rangle$. $|1_c, 1_t\rangle$ is denoted as the biexcitonic state. Measurements were conducted in 6K.

To study the biexciton, a laser was used to produce a strong pre-pulse (E_{pre}) that could tune into the exciton transition to prepare the qubit in the $|10\rangle$ state (Figure 7 b). A second laser, in the usual pump and probe geometry mentioned in section 2.1, manipulated the state and probed the result. When the pump and probe were scanned in frequency, a peak at the lower energy end of the spectrum appeared (Figure 7 a). This peak resonance corresponds to the biexciton transition related to the exciton that was excited by the pre-pulse.

Figure 8(a) shows one complete Rabi oscillation in the energy domain. The peak and the

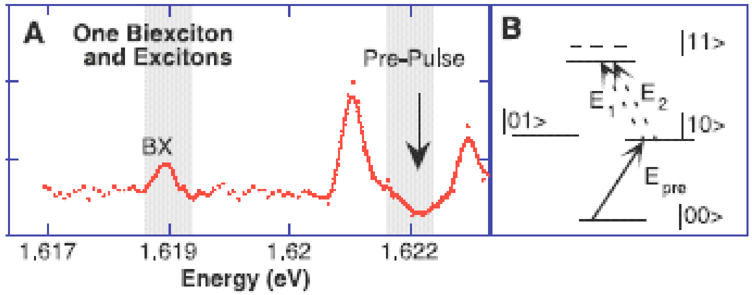

Figure 7: (a and b) The spectrum and experimental configuration with a pre-pulse tuned to one exciton transition and the biexciton (BX) state appearing at the lower energy end [20].

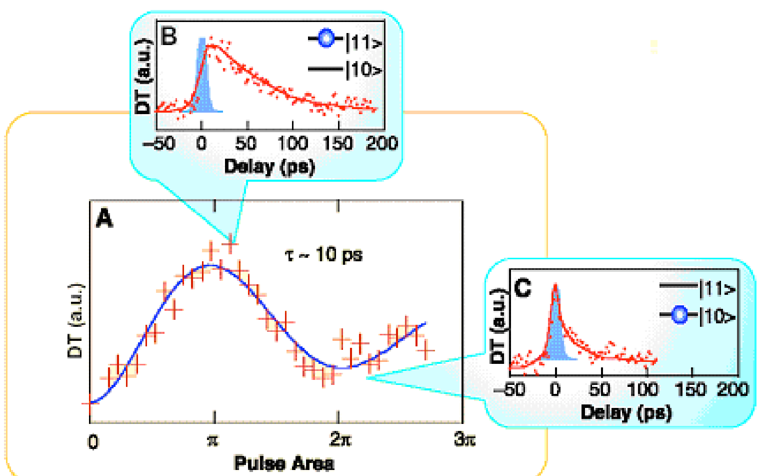

Figure 8: Biexcitonic Rabi oscillations. (a) Measured differential transmission (DT) vs the pulse area at fixed time delay τ 10ps, a sine-squared function with exponentially decaying amplitude (b and c) DT vs. time delay at fixed pump powers. The target states that follow the pump pulse are shown in the upper right, where the circles represent the exciton population [20].

trough correspond to pulse areas of $\sim \pi$ and $\sim 2\pi$, respectively. Around these two points, the pump power was fixed and the Rabi oscillation was observed this time as a function of probe delay, τ. The quantum states that followed the pump pulse in Figure 8(b) and 8(c) correspond to $-|11\rangle$ and $-|10\rangle$, respectively.

Thus, applying a π-pulse can be used as an operational pulse for the CROT gate from $|10\rangle$ to $|11\rangle$. If the input gate is $|00\rangle$, the operational pulse will be off-resonant and the output will remain $|00\rangle$. If the input is $|01\rangle$, the operational pulse will have the wrong polarization and the output will also remain the same [24]. However, when the input is $|10\rangle$, the operational pulse rotates to $-|11\rangle$. Similarly, if the input is chosen to be $|11\rangle$, the operational pulse stimulates it down to $|10\rangle$.

It is important to note that long pulses around 5 ps were used to avoid exciting multiple excitons under the same aperture. However, smaller apertures or different samples with more isolated QDs can be used to replace the long pulses with shorter ones. It is known that short dephasing times and long operational pulses force the fidelity (F) of the gate to be less than 1 ($F = 1$ only for ideal gates). X.Li et al, have calculated the overall fidelity of the CROT gate to be ~ 0.7 [25]. This system, however, is not scalable for an arbitrary number of qubits. Other schemes such as QDs attached to a linear support [25], or doped QDs coupled through exchange interactions [26] are promising scalable systems that could replace X.Li's et al, high fidelity CROT gate.

3 Hydrogenic Spin Quantum Computing in Silicon

The Hydrogenic Spin Quantum Computer uses electron-nuclear spin pairs as qubits [27]. This model can be thought of as a hybrid between quantum dot and NMR computing. The most promising feature of this proposal is that it uses the silicon-based solid state device. This is very big advantage over other proposals because 50 years of silicon research gave us a lot experience in manufacturing silicon so that this proposal is very realizable.

3.1 Implementation of quantum logic

As we can see from the Figure 9, phosphorus 31 P+ donors are located beneath the surface of the silicon substrate. The electrode A and S control the voltage between Si substrate surface and metal gates, which are separated by the barrier. We can also control the external magnetic field, Bglobal.

The coupling between the electron and 31 P+ Donors are modulated by changing the voltage on the A electrode. When there is a high voltage, electron is pulled toward the surface of the silicon substrate. So, there is no coupling. But when the voltage is low, 31 P+ donors couple strongly with electrons. When the nuclei spin couples with the electron spin, we can observe the hyperfine interaction. Hyperfine interaction is the coupling between electron spin and nucleus spin that leads to small perturbation to the basic atomic energy level because of the coexistence of the nuclear spin and electron spin. The nuclear spin interacts with the electron spins by dipole-dipole magnetic interaction. As the result, the evolution of nuclear

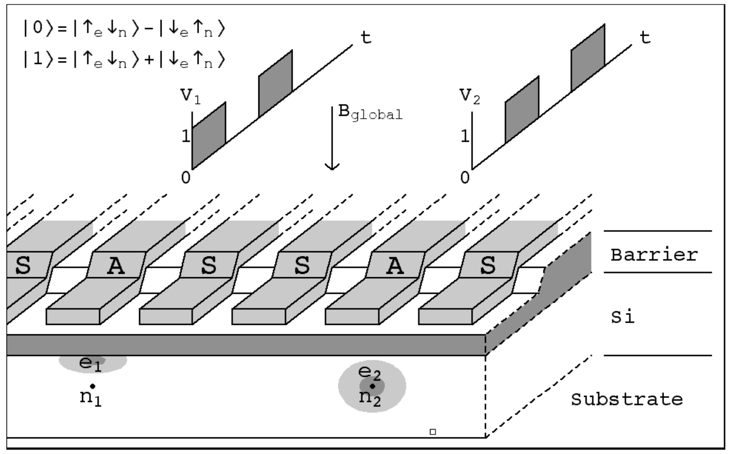

Figure 9: Schematic of the proposed architecture [27].

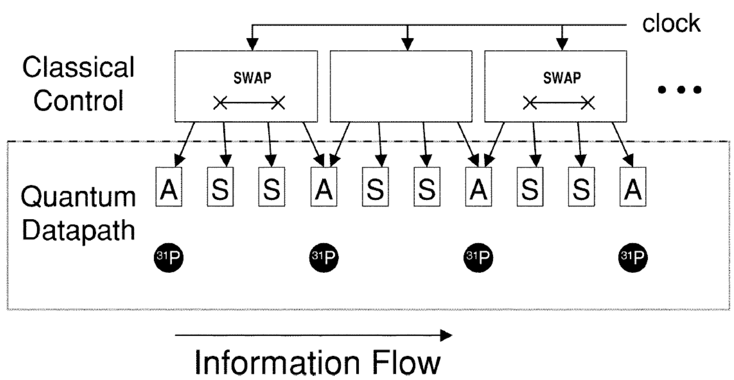

Figure 10: Swapping channel quantum data path [29].

and electronic spins are intertwined together and the Hamiltonian equation, which describes the time-evolution of the electron and nuclear spins, are governed by the external magnetic field.

The single qubit operation can be implemented by (1) controlling the coupling between the electron and donor nucleus which leads to the rotation of electron-nuclear paired qubit through x axis on the Bloch sphere, and (2) applying the external static magnetic field which leads to the rotation of paired qubit through z axis.

Two-qubit operations are done by electron shuttling between the adjacent A gates. S gates modulate this electron shuttling. This electron shuttling is called Heisenberg interaction , which allows us to build two qubit gates whose combination can make an universal quantum gate. For the further detail about the quantum mechanical explanation about the Heisenberg interaction [27, 28].

3.2 Transportation of data

We can transmit the quantum information by using swapping operation. The data-path is called the swapping channel. By controlling A and S electrode, we can implement the swapping operation. In order to build very scalable computer using the swapping channel , we need to consider three factors: the manufacturing possibility, the scale of classical control and the temperature. Following is the summary of these three technological challenge that Chuang points out [30].

The critical technological challenge in manufacturing is to place 31 p donors in the accurate position with 60nm interval with other donor below the metal gate. Current ion implantation technology or DNA-based self assembly technique can be used to do this task.

The second challenge is the scale of the classical controller. Current silicon processing technology does not reliably provide 10 nm width of controller line.

The third challenge is the heat. In order to preserve the coherence of the spin, we need to lower temperature. However, this low temperature causes several problems in the classical circuit. The classical circuit channel comes to shows the quantum mechanical characteristics as it reaches the low temperature. So, currently there is active research on making a transistor thats working in the low temperature, especially the single molecule transistor [29, 30]

Overall, the speculation of transporting data makes us think about what is really needed to implement the real scalable quantum computer. To further read about the challenge and analysis from the computer architecture point of view, read Chuang's paper [30].

4 Electron Spin

When contemplating any information processing system, either quantum or classical, it is first necessary to decide how information is going to be stored within the system, and how the system will process that information to perform the desired computation. Today, classical computation is typically carried out on microelectronic circuits that store information using the charge properties of electrons. Information processing is carried out by manipulating electrical fields within semiconductor material in such a way as to perform useful computational tasks.

Electrons possess a quantum physical property called spin; specifically electrons are spin-$\frac{1}{2}$ particles, which means that they have two orthogonal spin states, either spin up ($\frac{1}{2}$) or spin down ($-\frac{1}{2}$). This two level system is an obvious candidate for storing quantum information.

Experiments that have been conducted on quantum spin dynamics in semiconductor materials demonstrate that electron spins have several characteristics that appear promising for electron spin applications in quantum information processing. The dephasing time of electron spins in semiconductors has been reported to be as large as 100 ns [31]. This discovery is quite promising because longer decoherence times relax constraints on the switching speeds of quantum gates that is necessary for reliable error-correction. It is necessary that the quantum gates are able to switch 10^4 times faster then the individual qubits lose coherence [9]. Spin coherent transport over lengths as large as 100 μm in semiconductors have

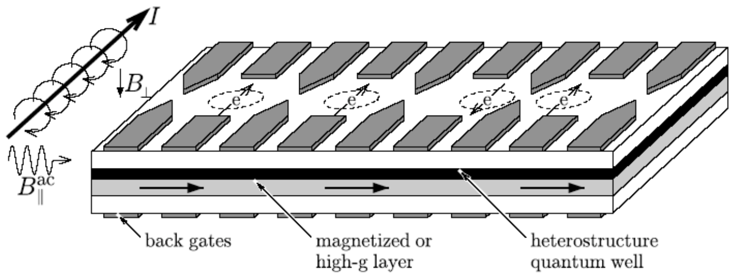

Figure 11: Theoretical proposal for defining quantum dots by using electrical gating. [33]. The magnetic fields shown in the diagram are representative of an ESR technique [35] for single-spin rotation.

been reported [31], which creates the potential use of electron spins as mobile information carriers in semiconductors.

4.1 Theoretical Proposals

Some of the initial theoretical work on electron spin quantum computation in quantum dot systems was done by Loss and Divincenzo[32], their work has been continued and expanded upon by Golovach and Loss [33]. Golovach and Loss's proposed implementation uses quantum dots that are defined within a two-dimensional electron gas (2DEG) by using appropriate electrical gating of a semiconductor quantum well (Figure 11). Other proposals using all-optical techniques have also been made, but will not be reviewed here [34].

4.2 Quantum gates

Quantum operations can potentially be performed using a variety of methods in this scheme. One-qubit operations are executed through single-spin rotations. One method to achieve this would be to expose a specific qubit to a time-varying Zeeman coupling [35]:

$$(g\mu_B \mathbf{S} \cdot \mathbf{B})(t) \tag{2}$$

The coupling can be controlled by varying the g-factor g or by manipulating the applied magnetic field $\mathbf{B}$ (μ_B is the Bohr magneton). Only the relative phases of the spins matter when using them to perform quantum computation so it would be possible to effect a single-spin rotation by rotating all the spins (eg. by processing them around an external magnetic field) but at different Larmor frequencies thereby causing the desired phase shift.

Another method for implementing a single-spin rotation in the Golovach-Loss proposal is to develop a method for applying localized magnetic fields over specific quantum dots. This could be achieved using an addressable array of current carrying wires. The dots would have be separated by enough distance to insure that neighboring bits were not affected. A magnetic disk writing head, or a magnetic scanning force microscope tip could also be used to create the necessary localized magnetic fields, but these implementations will become less feasible as the number of qubits increases since the operation speed will be limited by the positioning speed of the microscope tip, or magnetic head. There are other techniques for inducing a single-spin rotation in the quantum dot, such as ESR techniques [35] where an applied ac magnetic field with a resonant frequency matching the Larmor frequency of the qubit that will be flipped is applied perpendicular to the static magnetic field, as shown in Figure 11.

In order to form a universal set of gates our quantum computer will also need a two-qubit gate as well as the single-qubit gate created by single-spin rotation [36]. To form a two-qubit gate the exchange coupling between two adjacent quantum dots is employed. The low-energy dynamics of this system can be described by the effective Heisenberg spin Hamiltonian [32]:

$$H_s(t) = J(t)\mathbf{S_1} \cdot \mathbf{S_2} \tag{3}$$

where $J(t)$ is the exchange coupling between two spins denoted by $\mathbf{S_1}$ and $\mathbf{S_2}$. Appropriately pulsing $J(t)$ will interchange the qubits 1 and 2 [32], effectively performing the 'swap' operator U_{SW}. The 'swap' operator, while useful as we will see later on, is not sufficient to form a universal set of gates, but the square root of 'swap', $U_{SW}^{1/2}$ is. The $U_{SW}^{1/2}$ operator is defined as follows:

$$U_{SW}^{1/2}|\phi\chi\rangle = \frac{|\phi\chi\rangle + i|\phi\chi\rangle}{1+i} \tag{4}$$

The universality of $U_{SW}^{1/2}$ can be demonstrated by constructing the known universal gate XOR [37] by an appropriate sequence of $U_{SW}^{1/2}$ and single-qubit operation [32].

Theoretical models of the exchange mechanism have been investigated [33] and it is expected that $J(t)$ can be sufficiently controlled by adjusting the tunneling barrier between the quantum dots. By adjusting the depletion voltage, and bias voltage appropriately the size of the quantum dots as well as the tunnel bias can be controlled in such a way as to effect the necessary changes in $J(t)$ [32, 33]. The experimental details of such control have not yet been reported to our knowledge.

4.3 Quantum circuits

With a basic understanding of how a universal set of gates is formed in the Golovach-Loss proposal we can now see how a simple, scalable, all-electrical quantum circuit could be formed. The quantum dots could be aligned serially as shown in Figure 11. Although computation can only be performed on neighboring qubits in this scheme, the 'swap' operator can be used to move any two qubits next to one another to perform computation. This serial scheme is not as efficient as a parallel approach to quantum computing, but given the relative simplicity in the serial scheme, and the current state of quantum computers it is a valuable step towards the realization of a solid-state quantum computer.

Simply demonstrating how a gate operates is but one step in the design of a quantum circuit. As DiVincenzo points out other requirements need to also be met [7]. Again these five requirements are as follows: (i) identification of well-defined qubits, (ii) reliable state preparation, (iii) low decoherence, (iv) accurate quantum gate operations, and (v) strong quantum measurements.

We have already explained how (i), and (iv) are implemented in the Golovach-Loss proposal and hinted at (iii), but we have yet to discuss how to reliably prepare the states of the and perform strong quantum measurements.

As explained above, the gate operations for the Golovach-Loss are performed electrically through a use of a conversion through a spin-to-charge conversion, which is possible because of the Pauli exclusion principle and the Coulomb interaction. This conversion allows for very fast switching times on the order of picoseconds [33]. With gates speeds on the order of 10^1 picoseconds, and with spin coherence times of 100 ns [31] it looks promising that a electron spin scheme would be able to achieve the 10^4ratio between coherence time and switching speed necessary for reliable quantum error correction [9]. If these requirements can be met, the computation in the Golovach-Loss scheme should be stable.

It should be noted that since the circuit is serial the amount of operations dedicated to error-correction will require an increasing amount of computational overhead as the amount of qubits increases. Eventually a parallel quantum circuit will be desirable in order to decrease the computational load of error-correction.

To accurately prepare the initial states of the qubits the system need only be sufficiently cooled in a uniform applied magnetic field [32]. From a completely polarized system, any initial state can be reached by the appropriate application of single-spin rotation, as discussed above.

Lastly we need to discuss how to make measurements. There are two methods for performing single spin measurements, either through spontaneous magnetization, or by using another technique that allows the quantum dot to act as a spin filter or read-out/memory device.

Spontaneous magnetization is achieved by tunneling the electron to a supercooled paramagnetic dot [32]. This should have the effect of creating a net magnetization in the direction of the spin that can be read using conventional means. One problem with this form of measurement is that since the direction of the magnetization is continuous measurements can only be performed to 75% reliability [33].

The quantum dot can also be connected to two current carrying leads and operated as either a spin filter or a read-out/memory device with information being stored on a single spin [38]. The central idea to this scheme is to measure tunneling currents between the leads, which will be affected by the spin state within the quantum dot.

In order to realize such a system materials with different g-factors must be used for the leads and the quantum dot, so that the Zeeman splitting due to an external magnetic field is different between the dot and the leads. Therefore Coulomb blockade peaks and spin-polarized currents are uniquely associated with the spin state within the quantum dot. The tunneling current is made of two distinct components, the sequential current and co-tunneling current, in the Coulomb blockade regime that this technique operates within.

The spin filter operation is easier to explain so we will begin with that. In order to work effectively the system must be subject to the following constraints [38]:

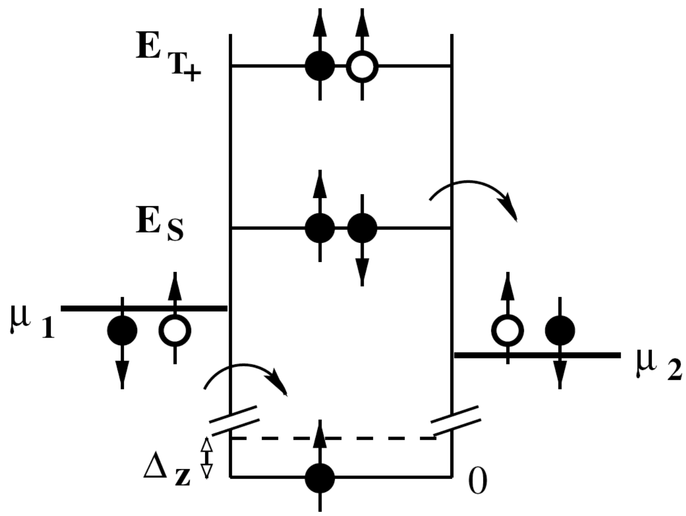

Figure 12: This energy diagram which is taken from [38] represents the energy levels of a quantum dot attached to two leads in the regime where the quantum dot contains an odd number of electrons. The topmost single electron in the ground state is considered to be spin up with energy $E_{\uparrow}$. The arrows depict a co-tunneling process where two possible virtual states, the singlet E_S and the triplet E_{T_+}, are shown. By using a gate voltage $E_S - \mu_1$ can be tuned to get into the sequential tunneling regime, which is defined by $\mu_1 \geq E_S \geq \mu_2$. Thus the number of electrons on the quantum dot fluctuates between odd and even, during the sequential tunneling regime. When the number of electrons on the quantum dot is even the ground state contains a topmost single state with $E_S < \mu_1, \mu_2$.

- Zeeman splitting within the leads is negligible (that is smaller then the Fermi energy) while the quantum has Zeeman splitting given as $\Delta z = \mu_B |gB|$.
- There must be a small bias $\Delta\mu = \mu_1 - \mu_2 > 0$ between the two leads at chemical potential $\mu_{1,2}$.
- Low temperature so that $\Delta\mu, kT < \delta$, where δ is the characteristic energy-level distance of the quantum dot.

Now consider the regime shown in Figure 12 where the quantum dot is in the ground state with an odd number of electrons with total spin $\frac{1}{2}$ and that the electron is $|\uparrow\rangle$ with energy $E_{\uparrow} = 0$. Now if an electron from one of the leads were to tunnel onto the quantum dot a spin singlet with energy E_S would be formed; the spin triplets are usually excited states with energies $E_{T_{\pm}}$ and E_{T_0}. For sequential tunneling resonance, where $\mu_1 \geq E_S \geq \mu_2$, the number of electrons fluctuates between odd and even numbers. If $E_{T_+} - E_S,\ \Delta z > \Delta\mu, kT$ then energy conservation will only allow ground state transitions. Therefore spin-up electrons are not allowed to tunnel onto the quantum dot because is would require either state E_{T_+}, or $|\downarrow\rangle$. Thus all the sequential current tunneling from lead 1 to lead 2 through the quantum dot is spin polarized $|\downarrow\rangle$. A spin polarized $|\downarrow\rangle$ sequential current be achieved in a similar fashion [38].

It should be mentioned that there is a small leakage current that arises from co-tunneling processes, but this has been shown to be small when compared to the sequential current [38].

For spin read-out the leads should be fully spin polarized, and the Zeeman splitting on the quantum dot should be much smaller. Experiments that have demonstrated that it is possible to tunnel inject spin polarized currents into an unpolarized GaAs system [39, 40], and tunnel injection could be achieved in a similar way here. The spin polarized currents tunneling through the dot will vary with the spin state of the quantum dot, assuming that there are an odd number of electrons on the dot. This phenomena occurs via a similar method as explained above for the spin filter with minor changes to the mathematics that describe the process [38].

To create a spin memory device ESR techniques [35] can be used to write the qubit inside the quantum dot: that is orient the spin of the electron either up or down. The qubit can be subsequently read and refreshed at a rate faster then the decoherence time.

5 Polarons - Phonon Mediated Decoherence

Physical implementations of qubits using Quantum Dots are fundamentally limited by the interaction of the qubits with their environment and the dephasing. These interactions of the qubits set the maximum time of coherent operation and an upper boundary for the number of quantum gate operations to be applied on a single qubit; therefore understanding the origin of decoherence is critical to control or reduce it, in order to implement quantum logic gates. (see [41] for calculated spin relaxation rates) Because of their strong localization in all directions, electrons confined in quantum dots are strongly coupled to longitudinal optical (LO) vibrations of the underlying crystal lattice. If the coupling strength exceeds the "continuum width" the energy of keeping the LO phonons delocalized a continuous Rabi oscillation of the electron arises, that is, an everlasting emission and absorption of one LO phonon. As a result, electron-phonon entangled quasi-particles known as polarons form; these play a substantial role in the rapid decoherence of the spin-based quantum dot qubits [42].

According to Wikipedia [42], a phonon is a quantized mode of vibration occurring in a rigid crystal lattice, such as the atomic lattice of a solid. Phonons account for many of the physical properties of solid state materials, such as conduction of sound in all solids, or of heat in insulators.

A crystal lattice is a rigid environment, in which atoms are kept around an equilibrium position by the forces they exert on each other; the net force is a combination of Van der Waals forces, electrostatic interactions and covalent bonds. Due to these almost-rigid connections between atoms, the displacement of one or more atoms from their equilibrium positions will give rise to a set of vibration waves propagating through the lattice.

Any vibration of a lattice can be decomposed into a superposition of normal modes of vibration. These are special cases of resonance in which all parts of the system oscillate

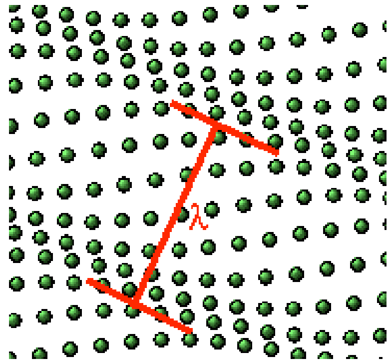

Figure 13: A longitudinal vibration (sound wave) propagating through a crystal lattice (reproduced from Wikipedia.org)

with the same allowed frequency. In a quantum dot, these frequencies of the normal modes determine two domains: the transverse (TO) and longitudinal (LO) optical modes.

The Q.M. treatment regards vibrational modes as phonons, particles with zero spin (hence bosons); such particles exist in all crystal lattices, but are confined inside Quantum Dots, much like electrons. Therefore, the interaction between phonons and electrons is the single most abundant interference event inside Quantum Dots, and will account for the decoherence of QD-based quantum logic systems. As mentioned before, error correction schemes require the ratio of the decoherence time to the time needed for one elementary operation to be at least 10^4.

Polarons themselves decohere very quickly (on the ps scale) because of the inelastic scattering of their optical phonon component by acoustical phonons of the underlying semiconductor lattice. In a recent paper, Zibik et al. analyze the decay of polarons, and identify the two distinct ways (channels) for such decay to occur: one involves the formation of two longitudinal acoustical (LA) phonons, with an energy of $\hbar\frac{\omega}{2}$ each and with opposite momentum; the other one involves the formation of one LA and one transversal acoustical (TA) phonon. Their data suggests the former to be the case, while Jacak et al. (and [42]) assume the latter to be valid in bulk GaAs QD systems [43, 44].

While individual phonons can not be directly observed, several successful attempts have been made at characterizing the phonon modes inside Quantum Dots. Henderson et al [45] describe a a simple non-destructive technique based on Far-Infrared Reflectance spectroscopy, to identify the phonon modes. However, it is still immensely difficult to practically devise a strategy as to minimize the interaction of electrons with phonons. Hohenester and Stadler take a theoretical approach at the optimal control of phonon-mediated dephasing of quantum dot systems, and conclude that appropriate tailoring of laser pulses allows to promote the system from the ground state through a sequence of excited states back to the ground state without suffering significant dephasing losses [46].

Although still a technological challenge, we expect an implementation of quantum logic gates using Quantum Dots in the not-so-far future.

Thanks to André DeHon and the Caltech Staff for hosting the Computing Beyond Silicon Summer School and to the presenters that taught us throughout our time there.

References

[1] P Shor. Algorithms for quantum computation: discrete logarithms and factoring. In *35th Annual Symposium on Foundations of Computer Science, 1994 Proceedings.*, page 124. IEEE Press, November 1994.

[2] L K Grover. Quantum mechanics helps in searching for a needle in a haystack. *Physical Review Letters*, 79(2):325–328, July 1997.

[3] J J Cirac and P Zoller. Quantum computations with cold trapped ions. *Physical Review Letters*, 74(20):4091–4094, May 1995.

[4] C Monroe, D M Meekhof, B E King, W M Itano, and D J Wineland. Demonstration of a fundamental quantum logic gate. *Physical Review Letters*, 75(25):4714–4717, December 1995.

[5] Q A Turchette, C J Hood, W Lange, H Mabuchi, and H J Kimble. Measurement of conditional phase shifts for quantum logic. *Physical Review Letters*, 75(25):4710–4713, December 1995.

[6] I L Chuang, N Gershenfeld, and M Kubinec. Experimental implementation of fast quantum searching. *Physical Review Letters*, 80(15):3408–34111, April 1998.

[7] D P DiVincenzo. Topics in quantum computers. `/cond-mat/9612126`, December 1996.

[8] D Mermin. Lecture notes on quantum computation (physics 481-681, cs 483), chapter 1: Fundamental properties of cbits and qbits, 2004. Available at: *http://people.ccmr.cornell.edu/∼mermin/qcomp/chap1.pdf*.

[9] J Preskill. Reliable quantum computers. *Proceedings: Mathematical, Physical and Engineering Sciences*, 454(1969):385, January 1998.

[10] L Pavesi, L Dal Negro, C Mazzoleni, G Franzò, and F Priolo. Optical gain in silicon nanocrystals. *Nature*, 408:440–444, November 2000.

[11] Andrey Rogach. Quantum dot rainbow. Available at: *http://www.nanopicoftheday.org/2003Pics/QDRainbow.htm*.

[12] The Strouse Group. University of California Santa Barbara: Chemistry Department. The basics of quantum dots. Available at: *http://www.chem.ucsb.edu/∼strouse_group/*.

[13] L P Kouwenhoven *et al.* *Mesocopic Electron Transport*, volume 345 of *NATO Science Series*. Proceeding of the NATO Advanced Study Institute, 1996.

[14] D P DiVincenzo. The physical implementation of quantum computation. *Fortschr. Phys.*, 48:771, 2000.

[15] H Kamada. Quantum computating with qd excitons. *NTT Tech. Rev.*, 1:31, 2003.

[16] M Bayer and A Forchel. Temperature dependence of the exciton homogeneous linewidth in indium-gallium-arsenide/gallium-arsenide self-assembled quantum dots. *Physical Review B*, 65(041308), 2002.

[17] D Birkedal, K Leosson, and J M Hvam. Long lived coherence in self-assembled quantum dots. *Physical Review Letters*, 87:227401, 2001.

[18] D Deutsch, A Brenco, and A Eckert. Universality in quantum computation. *Proc. Roy. Soc. London Ser. A*, 474:969, 1995.

[19] T H Stievater, X Li, D G Steel, D Gammon, D S Katzer, D Park, C Piermarocchi, and L J Sham. Rabi oscillations of excitons in single quantum dots. *Physical Review Letters*, 87:133603, 2001.

[20] X Li, Y Wu, D Steel, D Gammon, T H Stievater, D S Katzer, D Park, C Piermarocchi, and L J Sham. An all-optical quantum gate in a semiconductor quantum dot. *Science*, 301:809, 2003.

[21] M A Nielsen and I L Chuang. *Quantum Computation and Quantum Information*. Cambridge University Press, 2000.

[22] D Gammon, E S Snow, B V Shanabrook, D S Katzer, and D Park. Homogeneous linewidths in the optical spectrum of a single gallium arsenide qauntum dot. *Science*, 273:87, 1996.

[23] P Hawrylak, G A Narvaez, M Bayer, and A Forchel. Excitonic absorption in a quantum dot. *Physical Review Letters*, 85:389, 2000.

[24] P Michler, A Imamoglu, M D Mason, P J Carson, G F Strouse, and S K Buratto. Quantum correlation among photons from a single quantum dot at room temperature. *Nature(London)*, 406:968, 2000.

[25] Available at: *www.sciencemag.org/cgi/content/full/301/5634/809/DC1*.

[26] K R Brown, D A Lidar, and K B Whaley. Quantum computing with quantum dots on quantum linear supports. *Physical Review A*, 65:012307, 2001.

[27] A Skinner, M Davenport, and B Kane. Hydrogenic spin quantum computing in silicon: A digital approach. *Physical Review Letters*, 90:087901–087905, 2003.

[28] J Levy. Universal quantum computation with spin-1/2 pairs and heisenberg exchange. *Physical Review Letters*, 89:147902–147905, 2002.

[29] K Likhareve. Single-electron devices and their applications. *Proceedings of the IEEE*, 87(4):606–632, April 1999.

[30] D Copsey, M Oskin, F Impens, T Metodiev, A Cross, F Chong, and J Chuang Kubiatowicz. Toward a scalable, silicon-based quantum computing architecture. *Journal of Selected Topics in Quantum Electronics*, 9(6):1552–1569, 2003.

[31] D D Awschalom and J M Kikkawa. Electron spin and optical coherence in semiconductors. *Physics Today*, 52(6):33, June 1999.

[32] D Loss and D P DiVincenzo. Quantum computation with quantum dots. *Physical Review A*, 57(1):120–126, January 1998.

[33] V N Golovach and D Loss. Electron spins in artificial atoms and molecules for quantum computing. *Semiconductor Science and Technology*, 17:355–366, March 2002.

[34] T Calarco, A Datta, P Fedichev, E Pazy, and P Zoller. Spin-based all-optical quantum computation with quantum dots: Understanding and suppressing decoherence. *Physical Review A (Atomic, Molecular, and Optical Physics)*, 68(1):012310, 2003.

[35] G Burkard, D Loss, and D P DiVincenzo. Coupled quantum dots as quantum gates. *Physical Review B*, 59(3):2070–2078, January 1999.

[36] D P DiVincenzo. Two-bit gates are universal for quantum computation. *Physical Review A (Atomic, Molecular, and Optical Physics)*, 51(2):1015–1022, February 1995.

[37] A Barenco, C H Bennet, R Cleve, D P DiVincenzo, N Margolus, P Shor, T Sleator, J A Smolin, and H Weinfurter. Elementary gates for quantum computation. *Physical Review A (Atomic, Molecular, and Optical Physics)*, 52(5):3457, March 1995.

[38] P Recher, E V Sukhorukov, and D Loss. Quantum dot as a spin filter and spin memory. *Physical Review Letters*, 85(9):1962–1965, August 2000.

[39] R Fiederling; M Keim; G Reusher; W Ossau; G Schmidt; A Waag; L W Molenkamp. Injection and detection of a spin polarized current in a light-emitting diode. *Nature*, 402(6763):787–790, 1999.

[40] Y Ohno; D K Young; B Beschoten; F Matsukura; H Ohno; D D Awschalom. Electrical spin injection in a ferromagnetic semiconductor heterostructure. *Nature*, 402(6763):790–792, 1999.

[41] M Alcaide and G E Marques. Electron spin-phonon relaxation in quantum dots. *Brazilian Journal of Physics*, 345(2B):705, June 2004.

[42] Quantum Dot Group homepage. Quantum information with self-assembled quantum dots. Available at: *http://pages.ief.u-psud.fr/QDgroup/quantuminformation.html*.

[43] E A Zibik et al. Polaron relaxation channel in indium-arsenide/gallium-arsendie self-assembled quantum dots. *Semiconductor Science and Technology*, 19:S316, 2004.

[44] L Jacak et al. Anharmonicity-induced polaron relaxation in gallium-arsenide/indium-arsenide quantum dots. *Physical Review B*, 2002:113305, 2002.

[45] D O Henderson. Surface-phonon characterization of *InP*, *GaP* and *GaAs* quantum dots confined in dielectric hosts. *J. Phys. D: Appl. Phys.*, 30:1432, 1997.

[46] U Hohenester and G Stadler. Quantum control of electron-phonon scatterings in artificial atoms. *Physical Review Letters*, 92:196801, 2004.